Polymer 158 (2018) 223–230

Contents lists available at ScienceDirect

Polymer

journal homepage: www.elsevier.com/locate/polymer

pH-responsive Capsaicin@chitosan nanocapsules for antibiofouling in marine applications

Wenhui Wang[a,1], Xiangping Hao[a,1], Shougang Chen[a,*], Zhaoqing Yang[a], Caiyu Wang[a], Ran Yan[a], Xiao Zhang[b], Hu Liu[c,e], Qian Shao[d], Zhanhu Guo[c,**]

[a] School of Materials Science and Engineering, Ocean University of China, Qingdao, 266100, China
[b] College of Chemistry and Molecular Engineering, Qingdao University of Science and Technology, Qingdao, 266042, China
[c] Integrated Composites Laboratory (ICL), Department of Chemical & Biomolecular Engineering, University of Tennessee, Knoxville, TN, 37996, USA
[d] College of Chemical and Environmental Engineering, Shandong University of Science and Technology, Qingdao, Shandong, 266590, China
[e] Key Laboratory of Materials Processing and Mold (Zhengzhou University), Ministry of Education; National Engineering Research Center for Advanced Polymer Processing Technology, Zhengzhou University, Zhengzhou, 450002, China

HIGHLIGHTS

- pH responsive capsaicin@chitosan nanocapsules were prepared by microemulsion.
- These nanocapsules presented cyclic stability under alternate pH.
- The changed structure of nanocapsules was caused by the protonation and deprotonation amino groups of chitosan.
- Stable pH response performance of nanocapsules prolonged the service time of outstanding antibacterial activities.

ARTICLE INFO

Keywords:
Chitosan
Nanocapsules
Bacterial adhesion

ABSTRACT

Capsaicin@chitosan nanocapsules (CAP@CS) were prepared by micro-emulsion method in this work. Through transition between protonation and deprotonation of pH sensitive amino groups in chitosan, capsaicin can be triggered for self-releasing by pH changes resulted from bacterial reproduction. The total amount of released CAP@CS at pH 4 is five times more than that at pH 8.5. The CAP@CS is able to maintain the pH responsive property after 15 cycles of dialysis at pH ranging from 4 to 8.5, indicating a good cycling stability of CAP@CS nanocapsules. The bacteriostasis efficiency of CAP@CS is still up to 82.23%, 81.13% and 80.43% against adhesion of *Escherichia coli* (*E.coli*), *Staphylococcus aureus* (*S.aureus*) *and Pseudomons aeruginosa* (*P.* aeruginosa), respectively, which is caused by the repeated protonation and deprotonation of amino groups in chitosan. The prepared CAP@CS nanocapsules enable a bio-driven, intelligent and pH responsive performance for antifouling in marine applications.

1. Introduction

In marine environments, the traditional methods against the growth of bacteria by pre-doping biocides into coatings would result in an early loss of the coating's antifouling function because of the poorly controlled release of biocides [1–6]. A promising solution is to achieve controlled-release of biocides through microencapsulation on demand nowadays [6–9]. Microencapsulation, i.e., encapsulating biocides through covalent linkages or physical interactions, could reduce the rapid release of biocides from the nanocapsules to the surroundings, and protect the encapsulated biocides from degradation [10–13]. Moreover, the condition of local environment around nanocapsules will change due to the secretions produced by bacterial metabolism, such as temperature, pH and enzyme activity [14,15]. The fabrication of intelligent nanocapsules which can respond to the stimulation from environment is needed in antifouling field to further prolong the service time of antifouling agents [16–20].

Many natural or synthetic polymers, surfactants and lipids have

* Corresponding author.
** Corresponding author.
E-mail addresses: sgchen@ouc.edu.cn (S. Chen), zguo10@utk.edu (Z. Guo).
[1] The first two authors contributed equally to this work.

https://doi.org/10.1016/j.polymer.2018.10.067
Received 2 August 2018; Received in revised form 20 October 2018; Accepted 28 October 2018
Available online 30 October 2018
0032-3861/

been employed as intelligent drug carriers to achieve responsive release of drugs in vivo or in vitro [21–26]. Polysaccharides have received increasing attention due to their remarkable biological and physical properties, including high biocompatibility, excellent biodegradability, low toxicity, as well as abundant availability [21,25,27]. For instance, chitosan, alginate and cellulose derivatives have been studied widely as pH responsive materials [28–30]. Gellan and xanthan gums present remarkable temperature-sensitiveness for the transition between an ordered helix structure at low temperature and a disordered coil state at high temperature [31]. Polysaccharides with disulfide bonds which can be cleaved to thiol groups by glutathione in the cells can achieve intracellular controlled release of drugs [32].

Cationic natural polysaccharide chitosan (CS) [33–39] possesses antibacterial properties due to its interactions between the positively charged amino groups and the negatively charged cell membranes of bacteria [40–43]. Moreover, nanocapsules made of CS exhibit a typical pH-responsive characteristic due to the inclusion of a large number of amino groups in the side chains [44–50]. Specifically, the dissociation constant (pKa) of CS is about 6.5 [51], the nanocapsules swell due to the protonation of amino groups for the environmental pH < 6.5. Deprotonation of amino groups occurs in alkaline environments, resulting in the shrinking of nanocapsules to prolong the service time of drugs [36,45,52–54]. Thus, CS nanocapsules have been highly pursued as smart drug delivery system in vivo or in vitro [25,37,55]. However, it hasn't been studied for delivery of biocides intelligently in marine application.

In marine environments, the local pH increase due to the secretions produced by bacterial metabolism [14,15] and CS nanocapsules will swell and release biocides on demand subsequently to prevent the biofouling in response to the increasing environmental pH. On the contrary, the capsules will maintain closed in the absence of bacterial adhesion. Consequently, the intelligent nanocapsules can prolong the service time of antifoulant. Thus, CS provides a promising material for antifouling in marine application to store and release biocides in a controllable way upon stimulation by environmental changes. Furthermore, antifouling property means preventing the settlement of fouling organisms by killing organisms including micro-organisms like bacteria, diatoms and algae spores; the other is macro-organisms like barnacles, mussels, and algae. Antibacterial properties as one of the key parts of antifouling can prevent the bacteria adhesion progress, avoiding the following process of algae and mussels growth effectively. Therefore, combining antibacterial material with pH responsive chitosan can impart great antibacterial properties to chitosan nanocapsules for the application in antifouling field.

Due to the increasing restriction of toxic antibacterial material such as organo-tin compounds [56], eco-friendly biocides such as natural compounds derived from plants and animals have been paid more attention [57,58]. Among these natural compounds, capsaicin (CAP) is an ideal biocide due to its remarkable bactericidal performance, environmental friendly properties and excellent biodegradability [59–62]. Furthermore, CAP, as typical negative charged biocide, can form stable complexes by electrostatic interaction between CS and CAP to prolong the release period [37,38]. It is expected that CAP as biocide loaded in pH-responsive CS nanocapsules has the capability for developing intelligent antibiofouling nanocomposites, which have not been studied yet.

In this study, micro-emulsion method was used to prepare the pH-responsive CAP@CS nanocapsules with a controlled ratio of chitosan to capsaicin. The self-release performance of CAP@CS nanocapsules in response to pH changes was evaluated by colony counting method in the environments containing *Escherichia coli* (*E.coli*), *Staphylococcus aureus* (*S.aureus*) *and Pseudomons aeruginosa (P.* aeruginosa) bacteria. An alternate cycling test was conducted to characterize the cyclic stability of CS@CAP nanocapsules under different dialysate (pH 4 and pH 8.5). The remarkable cycling stability of CAP@CS nanocapsules was studied and found to be caused by repeated protonation and deprotonation of amino groups in chitosan.

2. Materials and methods

2.1. Materials

Capsaicin and soybean lecithin with a purity > 98% were purchased from Macklin Biochemical Co. Ltd. (Shanghai, China). Chitosan (CTS) with the viscosity-average molecular weight of 1.0×10^6 and deacetylation degree of about 95% was purchased from Aladdin Chemistry Co Ltd. (China). Phosphate buffered solution (PBS) solution was prepared with NaCl, KCl, Na_2HPO_4 and KH_2PO_4 and the pH value of PBS was adjusted with hydrochloric acid and sodium hydroxide. Model bacteria *S. aureus* (ATCC25923), *E. coli* (ATCC9522) and *P. aeruginosa* (ATCC27853) were purchased from RiShui Biotech Co.Ltd (Qingdao, China). SYTO9/Propidium-Iodide (PI) BacLight Bacterial Viability Kit was purchased from Invitrogen (Eugene, Oregon).

2.2. Preparation of core-shell CAP@CS nanocapsules

Capsaicin with varied weights (1.6, 3.2, 6.4 mg) was dissolved in 30 mg/mL absolute ethanol (400 mL) containing lecithin to prepare an oil phase. 10 mg chitosan was dissolved in 20 mL acetic acid aqueous solution (1%, v/v) by stirring at room temperature to prepare the chitosan solution as the aqueous phase. These two solutions were mixed upon stirring for 2 h to prepare the oil in water (O/W) microemulsion by micro-emulsion method. The CAP@CS nanocapsules were obtained after being transferred into a dialysis bag (MD25 8000-14000D) and immersed in PBS (pH 8.5) for 12 h to eliminate free capsaicin.

2.3. Measurements of pH responsive performance of the prepared CAP @CS nanocapsules

To measure the pH responsive performance of the prepared CAP@CS nanocapsules, 5 mL suspension of the prepared nanocapsules after dialysis was transferred into a dialysis bag (MD25 8000-14000D) and immersed into 50 mL PBS with various pH values (i.e., 4, 5, 6, 7, and 8.5), respectively, at room temperature. Aliquots (3.0 mL) of the solution at varied time intervals were taken from the dialysates to measure the concentration of released CAP by monitoring the absorption peak located at 280 nm by UV–Vis spectrometry [63]. After the sampling solution was taken, 3.0 mL fresh PBS was added back to keep the total volume of the test solution constant. The total capsaicin molecules released through the dialysis membrane over time was calculated by Equation (1) [46]:

$$\begin{aligned} &Mi = C_i \times 55\ mL + \sum_{j=1}^{j=i-1} C_j \times 3\ mL \\ &M_A = (0.32\ mg/mL - Cs) \times 3mL \\ &\text{Cumulative releasing}\ (\%) = M_i/M_A \times 100\% \end{aligned} \quad (1)$$

where M_i (mg) is the total amount of released capsaicin from CAP@CS nanocapsules as of measurement i, C_i (mg/mL) is the CAP concentration of sample i (i = 1,2,3 …), $\sum_{j=1}^{j=i-1} C_j \times 3$ mL is the total quantity of capsaicin in previously extracted samples, C_S is the concentration of free CAP before dialysis, and M_A is the total quantity of encapsulated CAP.

The suspension of CAP@CS after dialyzing in the PBS solutions (pH 4–8.5) was diluted and the zeta potential and size distribution of the prepared nanocapsules were determined by Zetasizer Nano and dynamic light scattering (DLS), respectively.

2.4. pH-responsive antibacterial property of the prepared CAP@CS nanocapsules

The antibacterial property of dialysates with pH of 4, 5, 6, 7 and 8.5, respectively, was tested after dialyzing CAP@CS nanocapsules for 4 h

by the colony counting method. *S.aureus* and *E.coil* were chosen as the representative of Gram-positive and Gram-negative bacteria, respectively. *P.aeruginosa* has also been tested as the representative of marine bacteria. The initial concentration of bacterial was about 10^7–10^8 CFU/ml. The bacteria were cultured in a Luria Broth medium and incubated in a shaking incubator at 37 °C at a rotating speed of 110 rpm for 18 h. The bacterial suspensions with different dialysates (pH 4, 5, 6, 7 and 8.5) and the same volume of physiological saline were then incubated in a shaking incubator for another 18 h. After that, 20 μL suspension of each dialysate was spread on a solid medium plate after diluted 10^5 times for colony counting.

In addition, the LIVE/DEAD bacterial viability kit was also used to evaluate the antibacterial property for comparison [64]. *E.coli* bacterial suspension was chosen as representative and was dyed by a mixture solution of PI (i.e., red fluorescent dye for dead bacteria) and SYTO9 (i.e., green fluorescent dye for live bacteria). The color of bacteria was observed from a fluorescence microscope to distinguish the live and dead bacteria.

2.5. Recyclable performance of the prepared CAP@CS nanocapsules

The CS@CAP suspension placed in a dialysis bag was dialysed for 0.5 h in dialysate (pH 4). 3.0 mL dialysate was taken to analyze the concentration of released capsaicin by UV–Vis spectrometry. The dialysis bag was then transferred to another dialysate (pH 8.5) and dialysed for another 0.5 h 3 mL dialysate was taken to analyze the concentration of released capsaicin. The zeta potential and diameter of CAP@CS after each dialysate were also detected. The process of alternating dialysis in dialysates with different pH values was repeated 15 times subsequently.

2.6. Characterization of CAP@CS nanocapsules

The size and surface morphology of the prepared CAP@CS nanocapsules were characterized using a transmission electron microscope (Hitachi H-700, Japan). The interaction between CS and CAP was analyzed by Fourier transform infrared spectroscopy (FT-IR) IS-50 spectrometer (Nicolet America) with KBr discs. The Zeta potential of the core-shell nanocapsules was measured by Zetasizer Nano (Malvern Instrument, UK). The diameter distribution of the nanocapsules was detected by dynamic light scattering (DLS) Zetasizer Nano (Malvern Instrument, UK). The encapsulation efficiency and the pH responsive behaviors of the prepared nanocapsules were performed by Ultraviolet and visible spectrophotometer (UV–Vis) (U−3900H, Hitachi Ltd). The fluorescent live/dead stain images were investigated by confocal laser scanning microscope (ZEISS Scope. A1).

3. Results and discussions

3.1. Characterization of the prepared CAP@CS nanocapsules

Fig. 1 shows the TEM image and size distribution of the prepared CAP@CS core-shell nanocapsules. The nanospheres with 220 nm in diameter were observed. Meanwhile, the average size of 231 nm of the nanospheres determined by DLS (also called hydrodynamic diameter) is consistent with the results from the TEM observation. The larger size measured by DLS was due to the solvent effect at the hydrated state.

Fig. 2 shows the FT-IR spectra of CAP@CS, CS and CAP. The broad adsorption peak at 3500- 3300 cm^{-1} is ascribed to the N−H and O−H stretching vibration of CS in Fig. 2b [65], while the peak at 2880 cm^{-1} is attributed to the C−H symmetric stretching vibration. The peaks at 1656 and 1590 cm^{-1} are due to the N−H bending vibrations which belong to the amino groups [66]. The peaks at 1423, 1371 and 1318 cm^{-1} indicate the C−H bending vibration, and the peak at 1014 cm^{-1} indicates the C−O−C skeletal stretching. For the spectra of capsaicin (i.e., spectrum c), the peaks at 3300 and 3600 cm^{-1}

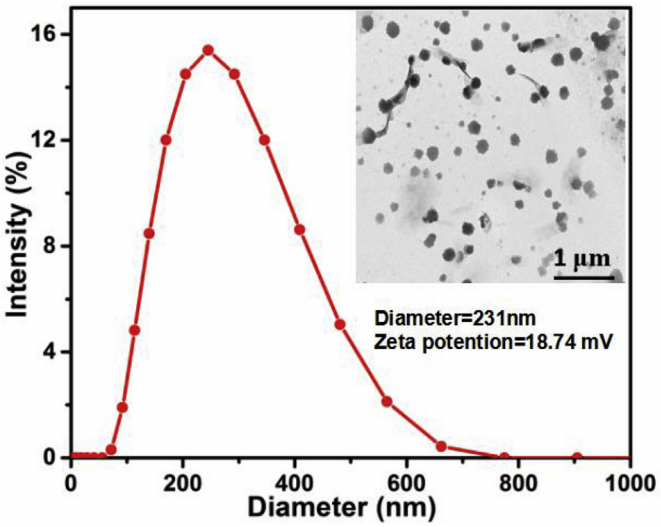

Fig. 1. TEM image and size distribution of CAP@CS core-shell nanocapsules. The diameter and zeta potential were detected in water solution (pH = 7).

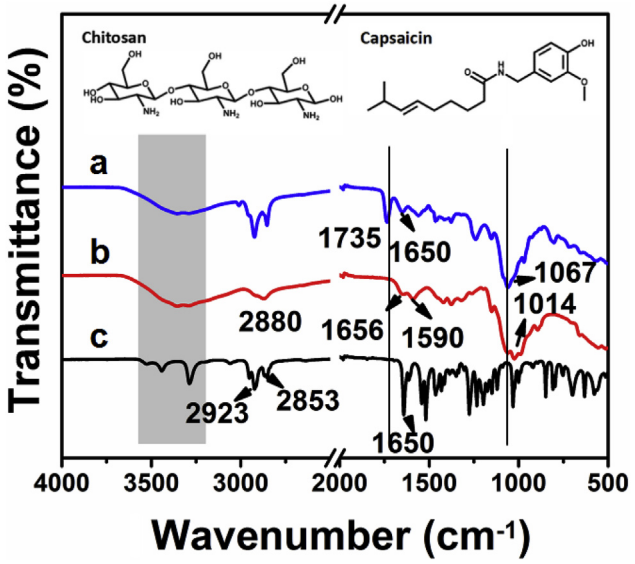

Fig. 2. FT- IR spectra of (a) CAP@CS, (b) CS and (c) CAP, respectively. The inset shows the molecular formula of chitosan and capsaicin.

correspond to the N−H stretching vibration and O−H stretching vibration, respectively. The peaks at 2853 and 2923 cm^{-1} are assigned to the C−H stretching vibration, and the peak at 1650 cm^{-1} is ascribed to the C=O stretching vibration [67]. For CAP@CS nanocapsules (i.e., spectrum a), the spectrum is similar to that of CS, while the peaks at 2853 and 2923 cm^{-1} correspond to the C−H stretching vibration of CAP. Meanwhile, the peak at 1650 cm^{-1} is ascribed to the C=O stretching vibration of CAP, indicating that CAP is contained in the prepared nanocapsules. Furthermore, the observed new absorption peak at 1735 cm^{-1} corresponds to the formation of hydrogen bonds between the carbonyl group of chitosan and the hydroxyl group of capsaicin [35], indicating the interaction between the chitosan and capsaicin.

The zeta potentials of CS, CAP and CAP@CS nanocapsules, as listed in Table S1, are +38.14, −11.28, and +18.74 mV, respectively. It is proven that the negatively charged surface of capsaicin is coated by positively charged chitosan. The results further confirm the interaction between chitosan and capsaicin, and are consistent with the results of FT-IR.

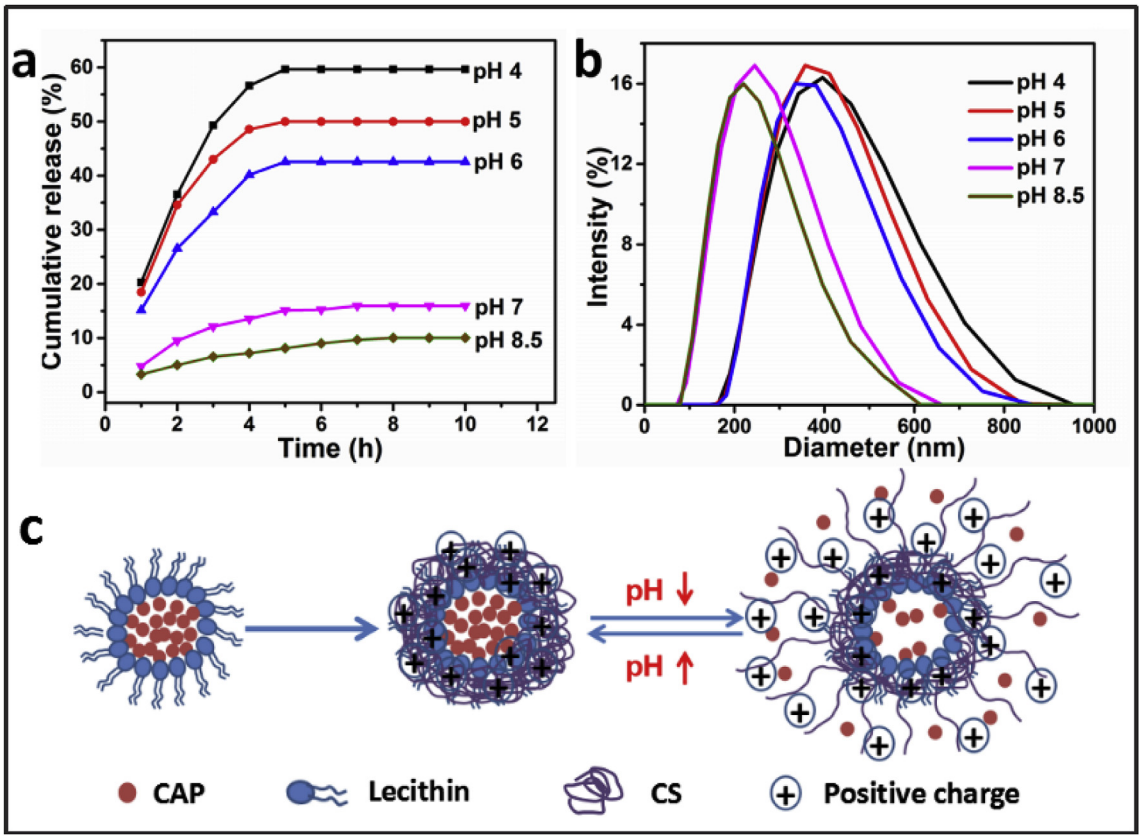

Fig. 3. Cumulative release of capsaicin under different pH conditions (a), size distribution of the CAP@CS nanocapsules under different pH conditions (b), and the proposed mechanism of the pH responsive releasing of CAP@CS nanocapsules (c).

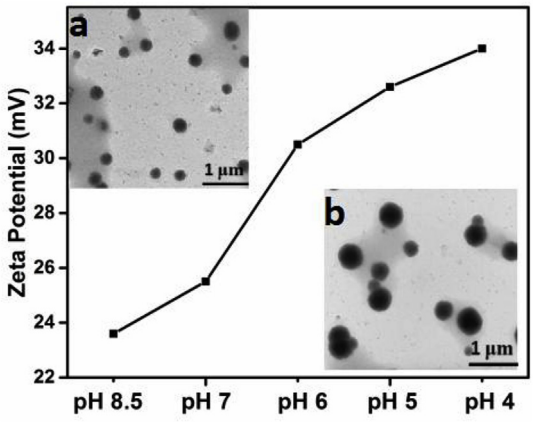

Fig. 4. The zeta potential of CAP@CS nanocapsules at varying pH values. Inset (a, b) are the TEM images of CAP@CS at pH 8.5 and pH 4 respectively.

3.2. pH responsive performance and mechanism of CAP@CS nanocapsules

Fig. 3a shows the cumulative percentage of released capsaicin in dialysate with various pH (4–8.5). The amount of released capsaicin was observed to increase with reducing the pH value. Initially, the amount of released capsaicin in dialysate (pH 4 and 5) increases rapidly, while that in dialysate of pH 7 and 8.5 increases slowly. At pH 4, the cumulative release of capsaicin increases to about 59.6%, triple times of 15.9% and 10.02% at pH 7 and pH 8, respectively. The cumulative release of capsaicin at pH 4 and 5 does not change after 4 h, while the released capsaicin at pH 7 and 8.5 reaches constant after about 9 h. Since bacterial reproduction can reduce the environmental pH, the release of capsaicin in response to the solution pH shows that the prepared CAP@CS nanocapsules provide a promising material triggered by bacterial activity for antibiofouling which will be tested in the next session.

The controlled release of CAP@CS nanocapsules is probably related to the structural change of the capsules upon treatment by dialysis solutions with various pH [45,51,52]. To further understand the structural changes of CAP@CS nanocapsules under different pH conditions, the size of the CS@CAP nanocapsules after dialysis in different dialysates (pH 4, 5, 6, 7 and 8.5) was measured by DLS, Fig. 3b. The calculated average sizes of the CS@CAP nanocapsules are 384, 352, 327, 231, and 212 nm under pH values of 4, 5, 6, 7 and 8.5, respectively. The increased size with the decrease of the dialysate pH is well consistent with the UV–Vis results. The increased hydrated size of CAP@CS under acidic conditions (e.g., pH 4 and 5.5) is due to the swelling of capsules by protonation of the amino groups, which facilitates the release of pre-stored capsaicin. With the increase of pH value, the capsules become smaller due to the deprotonation of amino groups. The smallest size of the capsules obtained at pH 8.5 is almost the same as that of the capsules without any release. Additionally, the TEM images of CAP@CS pH 4 and pH 8.5 were also detected and presented in the inset image of Fig. 4. The diameter of CAP@CS is 430 and 240 nm at pH 4 and pH 8.5, respectively and the morphology of CAP@CS remains stable at pH 4.

Based on the results of UV–Vis and DLS measurements, the mechanism for the pH responsive releasing behavior of CAP@CS nanocapsules is illustrated in Fig. 3c. Since the pKa of chitosan is about 6.5, the $-NH_2$ groups change to the $-NH_3^+$ groups with the protonation of amino groups when the pH of dialysate is decreased to pH 6, resulting in an increase of positive charges and the electrostatic interaction in system [36,45,53]. Since the amino groups are located on the side chain of chitosan, the diffusion channel of small molecules becomes large, promoting the release of capsaicin encapsulated in chitosan. Therefore,

both the release rate of capsaicin and the cumulative released amount increase with decreasing the pH value. When the environmental pH increases to pH 7, the polymer network starts to shrink due to the amino deprotonation, inhibiting the release of capsaicin. In addition, the maximum cumulative release of capsaicin can only reach 59.6%, it can be explained by the electrostatic interaction between chitosan and capsaicin.

To demonstrate the protonation process of amino groups on chitosan more intuitively, the zeta potential of CAP@CS after dialysis in different dialysates (pH 4, 5, 6, 7 and 8.5) was measured. Fig. 4 presents the values of zeta potential increased with the decreased pH values. The increasing zeta potential values indicates the changing from NH_2 to NH_3^+ at amino groups on chitosan through combining with H^+ in acid environment. On the contrary, NH_3^+ converts back to NH_2 through dehydrogenation under alkaline condition, leading to decreased zeta potential values. Hence, capsaicin can release from nanoparticles during the protonation process of chitosan. Therefore, this results of zeta potential can be combined with the results of DLS and releasing experiments to demonstrate the presence of structural changes in chitosan leading to its pH response performance.

3.3. pH-responsive antibacterial property of the CAP@CS nanocapsules

Fig. 5 shows the colony counting results and bacteriostasis of CS, CAP, and CAP@CS capsules against the adhesion of *E.coil*, *S.aureus and P. aeruginosa*. The bacteriostasis is calculated by equation (a) [68–71]:

$$Bacteriostasis = (A - B) \div A \times 100 \quad (2)$$

where A is the number of bacteria under control, and B is the number of bacteria of the experimental samples.

It is seen from Fig. 5 (a, b) that the capsaicin possesses an excellent antibacterial property. The bacteriostasis efficiencies against *E.coli*, *S.aureus and P. aeruginosa* are up to 98.21%, 98.79% and 98.91%, respectively. It is primarily attributed to the strong irritation of capsaicin to bacteria. The bacteriostasis efficiencies of chitosan against *E.coli*, *S.aureus and P. aeruginosa* are 82.88%, 76.47% and 84.71%, respectively. The antibacterial property of chitosan is ascribed to the positively charged amino groups which can kill bacteria through the interaction between the positively charged CS and the negatively charged bacteria. The results also demonstrate that CAP@CS nanocapsules are more effective for antibacterial adhesion than single CS

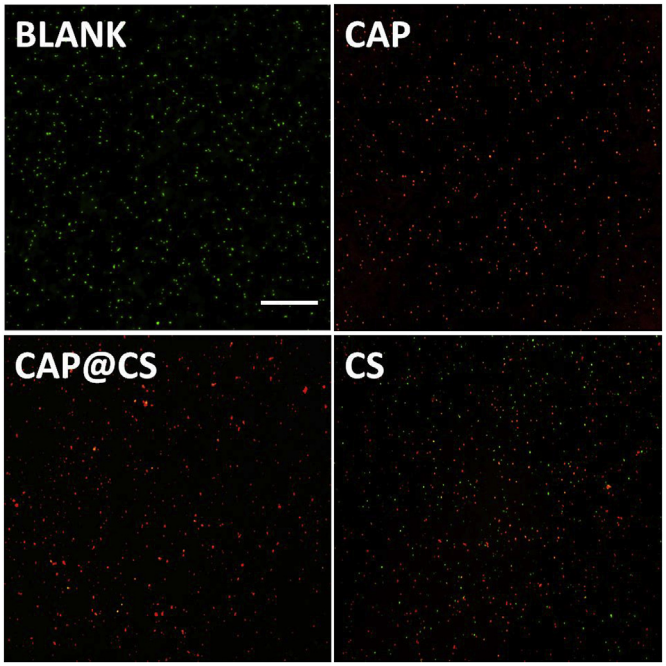

Fig. 6. Fluorescent live/dead stain images of BLANK, CAP@CS nanocapsules, CAP and CS. The *E.coli* bacteria suspension was incubated with physiological saline solution, CAP@CS, CAP and CS for 18 h respectively and was stained with the BacLight live/dead kit assay. Red and green dots refer to dead and live bacteria, respectively. The scale bar is 10 μm. The experiments were done with bacteria out of the culture directly and all tests were repeated at least 3 times. (For interpretation of the references to color in this figure legend, the reader is referred to the Web version of this article.)

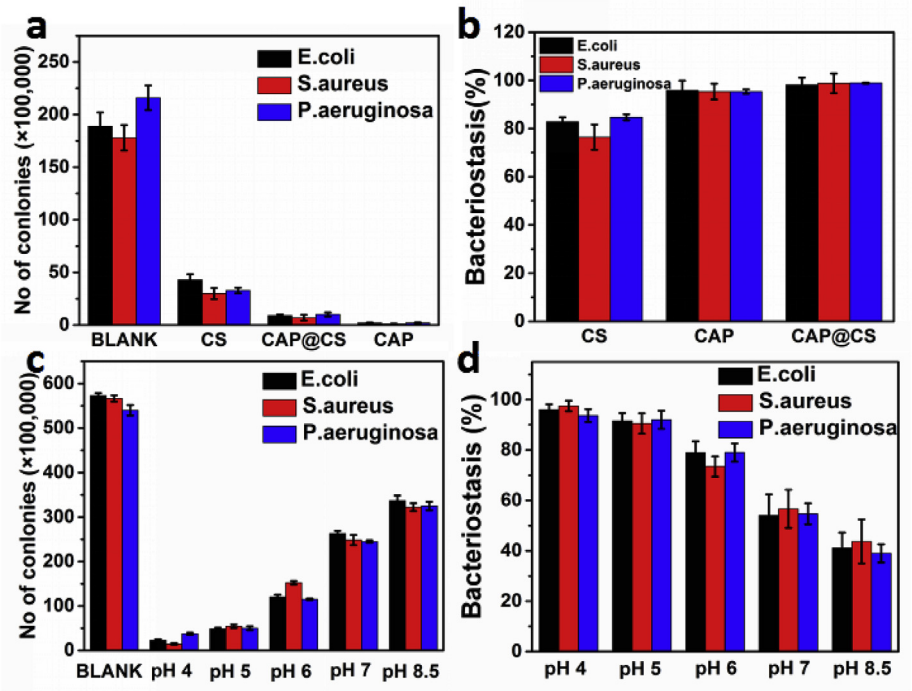

Fig. 5. The number of *E.coli*, *S.aureus, P. aeruginosa* and bacteriostasis of CS, CAP, CAP@CS (a) (b), and those as a function of pH of the dialysate (c), (d). The experiments were done with bacteria out of the culture directly and all tests were repeated at least 3 times.

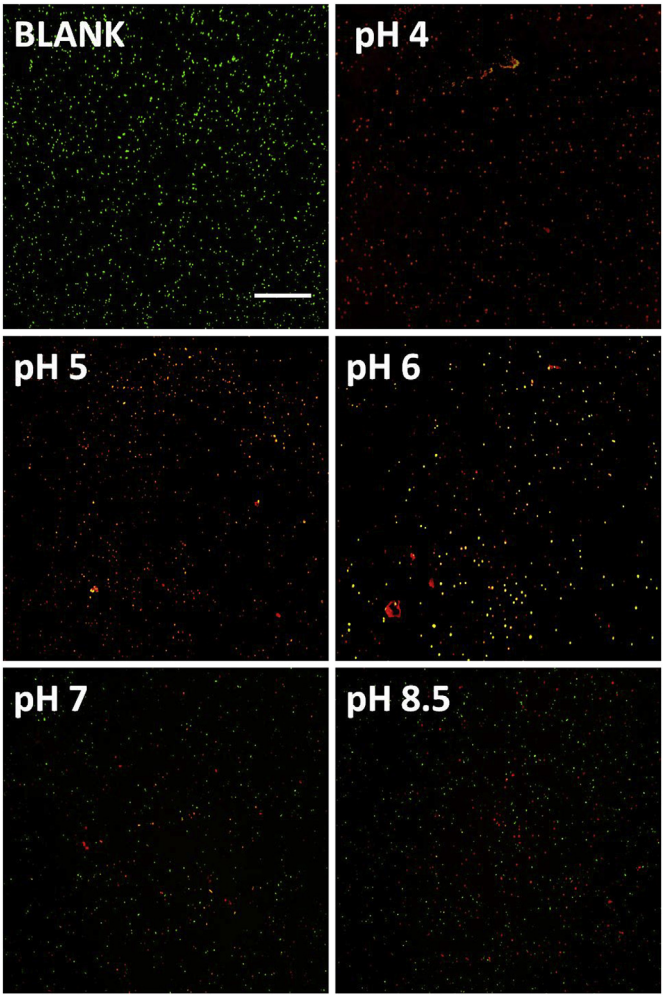

Fig. 7. Fluorescent live/dead stain images of BLANK, pH 4, pH 5, pH 6, pH 7 and pH 8.5 dialysates. The *E.coli* bacteria suspension was incubated with physiological saline solution, pH 4, pH 5, pH 6, pH 7 and pH 8.5 dialysates for 18 h respectively and was stained with the BacLight live/dead kit assay. Red and green dots refer to dead and live bacteria, respectively. The scale bar is 10 μm. The experiments were done with bacteria out of the culture directly and all tests were repeated at least 3 times. (For interpretation of the references to color in this figure legend, the reader is referred to the Web version of this article.)

sample, with 95.91%, 95.37% and 95.37% of bacteriostasis against *E.coli*, *S.aureus and P. aeruginosa,* respectively. The enhanced antibacterial property is partly due to the sustained release of capsaicin from the CAP@CS nanocapsules, and partly by the bactericidal properties of chitosan. Moreover, capsaicin is initially embedded in the capsule. It could not kill bacteria as quickly as pure capsaicin. With adhesion and growth of bacteria, the decreased solution pH around the nanocapsules causes the protonation of chitosan. The swelling effect of nanocapsules will cause capsaicin to release rapidly. Hence, the controlled release of capsaicin from the CS@CAP nanocapsules is in response to the pH change for antibiofouling.

To verify the pH-triggered antibacterial property of the CAP@CS nanocapsules, the bacteriostasis of dialysates with various pH values was tested by the plate count method as well. The results shown in Fig. 5 (b, d) demonstrate that, with the increase of the dialysate pH, the antibacterial effect of dialysate is reduced gradually. According to the proposed mechanism stated above, the bacteriostasis is achieved by the release of capsaicin from the nanocapsules with the decrease of the pH value of dialysate. At high pH values, the shrinkage of nanocapsules reduced the released capsaicin amount, resulting in a lower bacteriostasis.

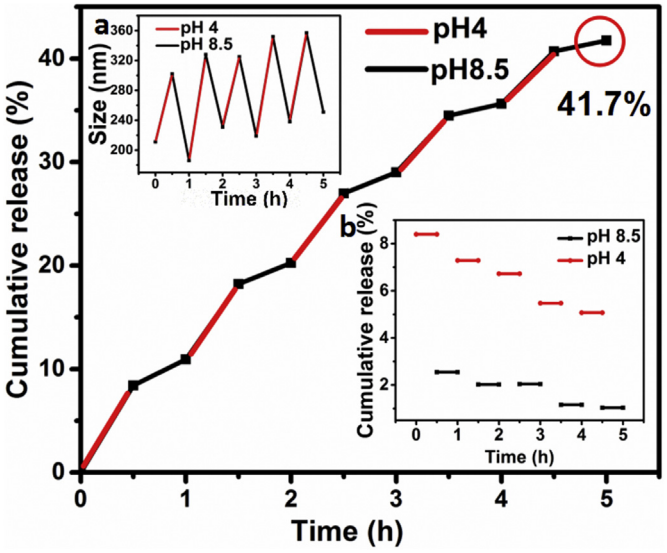

Fig. 8. Cumulative release percentage of CAP under alternate cycling test. Inset (a) shows the change of the diameter of CAP@CS under two pH values. Inset (b) shows the cumulative release of CAP during intervals (0.5 h) under different pH values.

The bacteriostatic effect can be seen directly from the fluorescence images in Figs. 6 and 7. It is seen that the capsaicin possesses the best antibacterial performance, and the CAP@CS nanocapsules show a better antibacterial property than pure chitosan. Moreover, the bacteriostasis of dialysate decreases with increasing the pH value. Since antibacterial property is one of the antifouling aspects which can restrict bacteria adherent and prevent the fouling process earlier, pH responsive CAP@CS with remarkable antibacterial property have great potential applications in antifouling.

3.4. Cyclic stability of the prepared CAP@CS nanocapsules

In reality, the pH value of the marine environment around the bioattached structures may change from alkaline/neutral to acidic with the multiplication of bacteria. After the bacteria are killed by the released biocides and removed from the structure surface, the environmental pH can change back to neutral/alkaline gradually. An alternate cycling test to simulate the release process of nanocapsules under pH 4 and 8.5 dialysates was conducted, Fig. 8. The amount of released capsaicin increases with increasing the time, and the cumulative release amount reaches 41.7% after 5 h. There are about 20% capsaicin saved compared to the result after dialyzing at pH 4 for 5 h. With increasing the pH value from 4 to 8.5, the capsaicin release becomes slower. Although the release rate of capsaicin decreases gradually as the number of cycles increases, which probably results from the reduced concentration of encapsuled capsaicin, the release rate at pH 4 is still higher than that at pH 8.

Furthermore, the size of nanocapsule particles after each cycle is measured by DLS and the results are shown in the inset (a) of Fig. 8. The average diameters of CAP@CS nanocapsules at pH 4 and 8.5 are about 320 and 220 nm, respectively, indicating the expansion of the nanocapsules at pH 4 and the shrinkage at pH 8.5. The bacteriostasis of CAP@CS nanocapsules after 5 alternate cycles performs well, with a bacteriostasis of 82.23%, 81.13% and 80.43% against *E.coli*, *S.aureus and P. aeruginosa*, respectively. It shows a great cycling stability of the CAP@CS nanocapsules, which contribute to the recyclable process of protonation and deprotonation.

To further demonstrate the cyclic stability of the CAP@CS nanocapsules, the process of placing CAP@CS in PBS solution with alternate (pH4 and pH 8) was repeated 15 times and the result was presented in

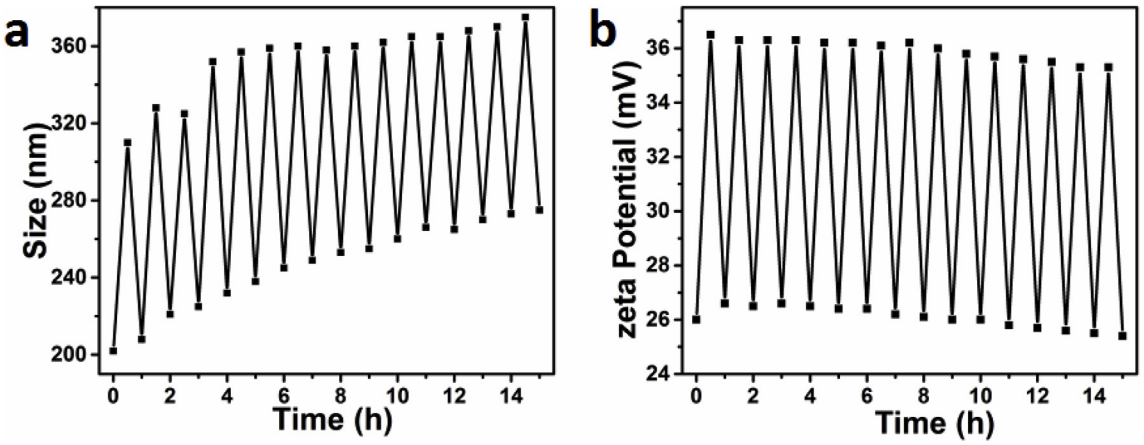

Fig. 9. The size change (a) and zeta potential values (b) of CAP@CS nanocapsules under alternate pH (pH 4 and pH 8.5) during 15 cycles.

Fig. 9. The sizes of CAP@CS which represent the swelling degree of nanocapsules are about 350 nm at pH 4 and 250 nm at pH 8.5 in 15 cycles, respectively, indicating that the pH response property can maintain for at least 15 times. This phenomenon is caused by the repeated protonation and deprotonation process of amino groups on the chitosan [36]. The amino groups on chitosan can change from NH_2 to NH_3^+ through combining with H^+ in acid environment. The electrostatic interactions of the positively charged ions can lead to segment rejection, which provides the release channel for capsaicin. On the contrary, nanocapsules shrink under alkaline condition with NH_3^+ converting back to NH_2 through dehydrogenation [48–50]. Therefore, the prepared CAP@CS nanocapsules can repeat pH response under alternate pH through repeated binding and desorption of hydrion. Additionally, the increased size of nanoparticles at pH 8.5 can be attribute to the swelling effect caused by long-term immersion in the buffer after cycles.

To further demonstrate the protonation and deprotonation process of chitosan and research the dispersivity and stability of CAP@CS nanocapsules, the zeta potential values of CAP@CS nanocapsules under alternate pH (pH 4 and pH 8.5) during 15 cycles were also detected. The results are presented in Fig. 9b. The results present that the zeta potential values were almost constant after 15 cycles, indicating that the protonation and deprotonation process of amino groups on the chitosan still remain stable. CAP@CS still possesses the ability to adsorb and desorb the hydrogen ions. The slightly decreased potential can be explained by the decreased stability of the system which is caused by the increased diameter of nanocapsules with long-term immersion in PBS. The result indicates that the CAP@CS nanocapsules can remain stable in the environment with alternate pH, which endows the CAP@CS nanocapsules with the potential to be used in marine antifouling applications.

4. Conclusions

The pH responsive CAP@CS nanocapsules with a high cycling stability and antibacterial property were successfully prepared as novel antifouling agents by microemulsion polymerization. Depending on the environmental pH being acid or alkaline, the nanocapsules can expand or contract due to the protonation or deprotonation of chitosan, affecting the release of capsaicin. The environmental acidification can be caused by bacterial reproduction in the marine environment, the release of capsaicin can be triggered by the changed pH. The antibacterial property of dialysate is found to increase with decreasing the pH value due to the release of capsaicin in the acidic environment. The CAP@CS nanocapsules maintained the pH responsive property, and demonstrated a considerable bacteriostasis after cyclic alternate dialysis under acid and alkali conditions with combined cyclic stability. The prepared pH responsive CAP@CS nanocapsules can serve as novel antifouling agents for marine antifouling.

Acknowledgements

This work was supported by the National Natural Science Foundation (51572249), the Key Research Project of Shandong Province (911861230), the Natural Science Foundation of Shandong Province (ZR2014EMM021, ZR2017MD016) and the Fundamental Research Funds for the Central Universities (841562011) and the Key Research Project of Shandong Province (911861230).

Appendix A. Supplementary data

Supplementary data to this article can be found online at https://doi.org/10.1016/j.polymer.2018.10.067.

References

[1] M.P. Schultz, J.A. Bendick, E.R. Holm, W.M. Hertel, Economic impact of biofouling on a naval surface ship, Biofouling 27 (2011) 87–98.
[2] J. Fang, A. Kelarakis, D. Wang, E.P. Giannelis, J.A. Finlay, M.E. Callow, J.A. Callow, Fouling release nanostructured coatings based on PDMS-polyurea segmented copolymers, Polymer 51 (2010) 2636–2642.
[3] E. Martinelli, C. Pretti, M. Oliva, A. Glisenti, G. Galli, Sol-gel polysiloxane films containing different surface-active trialkoxysilanes for the release of the marine foulant Ficopomatus enigmaticus, Polymer 145 (2018) 426–433.
[4] S. Chen, C. Ma, G. Zhang, Biodegradable polymers for marine antibiofouling: poly(ε - caprolactone)/poly(butylene succinate) blend as controlled release system of organic antifoulant, Polymer 90 (2016) 215–221.
[5] J. Bergek, M. Andersson Trojer, H. Uhr, L. Nordstierna, Controlled release of a microencapsulated arduous semi-hydrophobic active from coatings: super-hydrophilic polyelectrolyte shells as globally rate-determining barriers, J. Contr. Release 225 (2016) 31–39.
[6] M. Andersson Trojer, L. Nordstierna, J. Bergek, H. Blanck, K. Holmberg, M. Nyden, Use of microcapsules as controlled release devices for coatings, Adv. Colloid Interface Sci. 222 (2015) 18–43.
[7] S. Li, A. Jasim, W. Zhao, L. Fu, M.W. Ullah, Z. Shi, G. Yang, Fabrication of pH-electroactive bacterial cellulose/polyaniline hydrogel for the development of a controlled drug release system, ES Mater. Manuf. 1 (2018) 41–49, https://doi.org/10.30919/esmm5f120 www.doi.org/10.30919/esmm5f120.
[8] P. Zhang, T. Ge, H. Yang, S. Lin, Y. Cao, C. Zhao, H. Liu, A. Umar, Z. Guo, Antifouling of titania nanostructures in real maritime conditions, Sci. Adv. Mater. 10 (2018) 1216–1223.
[9] D. Aycan, N. Alemdar, Development of pH-responsive chitosan-based hydrogel modified with bone ash for controlled release of amoxicillin, Langmuir 184 (2018) 401–407.
[10] W. Shen, Y. Chang, G. Liu, H. Wang, A. Cao, Z. An, Biocompatible, antifouling, and thermosensitive Core – Shell nanogels synthesized by RAFT aqueous dispersion polymerization, Macromolecules 44 (2011) 2524–2530.
[11] M. Andersson Trojer, L. Nordstierna, M. Nordin, M. Nyden, K. Holmberg, Encapsulation of actives for sustained release, Phys. Chem. Chem. Phys. 15 (2013) 17727–17741.
[12] A. Fery, R. Weinkamer, Mechanical properties of micro- and nanocapsules: single-capsule measurements, Polymer 48 (2007) 7221–7235.
[13] L. Nordstierna, A.A. Abdalla, M. Masuda, G. Skarnemark, M. Nydén, Molecular release from painted surfaces: free and encapsulated biocides, Prog. Org. Coating 69 (2010) 45–48.

[14] D.M. Yebra, S. Kiil, K. Dam-Johansen, Antifouling technology—past, present and future steps towards efficient and environmentally friendly antifouling coatings, Prog. Org. Coating 50 (2004) 75–104.
[15] S.J. Kiprono, M.W. Ullah, G. Yang, Surface engineering of microbial cells: strategies and applications, Eng. Sci. 1 (2018) 33–45 http://www.doi.org/10.30919/es.180330.
[16] K. Sunada, M. Minoshima, K. Hashimoto, Highly efficient antiviral and antibacterial activities of solid-state cuprous compounds, J. Hazard Mater. 235–236 (2012) 265–270.
[17] F. Jiang, S. Chen, Z. Cao, G. Wang, A photo, temperature, and pH responsive spiropyran-functionalized polymer: synthesis, self-assembly and controlled release, Polymer 83 (2016) 85–91.
[18] Z. Hu, D. Zhang, F. Lu, W. Yuan, X. Xu, Q. Zhang, H. Liu, Q. Shao, Z. Guo, Y. Huang, Multistimuli-responsive intrinsic self-healing epoxy resin constructed by host−-guest interactions, Macromolecules 51 (2018) 5294–5303.
[19] P.M. Mendes, Stimuli-responsive surfaces for bio-applications, Chem. Soc. Rev. 37 (2008) 2512–2529.
[20] Y. Cong, K. Chen, S. Zhou, L. Wu, Synthesis of pH and UV dual-responsive microcapsules with high loading capacity and their application in self-healing hydrophobic coatings, J. Mater. Chem. 3 (2015) 19093–19099.
[21] C. Alvarez-Lorenzo, B. Blanco-Fernandez, A.M. Puga, A. Concheiro, Crosslinked ionic polysaccharides for stimuli-sensitive drug delivery, Adv. Drug Deliv. Rev. 65 (2013) 1148–1171.
[22] M. Andersson Trojer, L. Nordstierna, M. Nordin, M. Nyden, K. Holmberg, Encapsulation of actives for sustained release, Phys. Chem. Chem. Phys. 15 (2013) 17727–17741.
[23] F. Masood, Polymeric nanoparticles for targeted drug delivery system for cancer therapy, Mater Sci Eng C Mater Biol Appl 60 (2016) 569–578.
[24] K.M. El-Say, H.S. El-Sawy, Polymeric nanoparticles: promising platform for drug delivery, Int. J. Pharm. 528 (2017) 675–691.
[25] J.H. Park, G. Saravanakumar, K. Kim, I.C. Kwon, Targeted delivery of low molecular drugs using chitosan and its derivatives, Adv. Drug Deliv. Rev. 62 (2010) 28–41.
[26] Y. Ma, M. Ma, X. Yin, Q. Shao, N. Lu, Y. Feng, Y. Lu, E.K. Wujcik, X. Mai, C. Wang, Z. Guo, Tuning polyaniline nanostructures via end group substitutions and their morphology dependent electrochemical performances, Polymer 156 (2018) 128–135 https://www.doi.org/10.1016/j.polymer.2018.09.051.
[27] M.J. Cardoso, R.R. Costa, J.F. Mano, Marine origin polysaccharides in drug delivery systems, Mar. Drugs 14 (2016).
[28] M.K. Akihiko Kikuchi, Teruo Okanoa, Masayasu Sugihara, Yasuhisa Sakurai, Pulsed dextran release from calcium-alginate gel beads, J. Contr. Release 47 (1997) 21–29.
[29] O.S. Lawal, M. Yoshimura, R. Fukae, K. Nishinari, Microporous hydrogels of cellulose ether cross-linked with di- or polyfunctional glycidyl ether made for the delivery of bioactive substances, Colloid Polym. Sci. 289 (2011) 1261–1272.
[30] R. Barreiro-Iglesias, R. Coronilla, A. Concheiro, C. Alvarez-Lorenzo, Preparation of chitosan beads by simultaneous cross-linking/insolubilisation in basic pH. Rheological optimisation and drug loading/release behaviour, Eur. J. Pharmaceut. Sci. 24 (2005) 77–84.
[31] E.R. Morris, K. Nishinari, M. Rinaudo, Gelation of gellan – a review, Food Hydrocolloids 28 (2012) 373–411.
[32] C. Zhang, Y. Zhang, X. Hao, H. Liu, X. Lv, J. Zhu, W. Han, Y. Zhang, Fabrication of reduced graphene oxide/chitosan composite fiber by dry-jet wet spinning, Adv. Compos. Hybrid Mater. 1 (2018) 347–355.
[33] C. Choochottiros, R. Yoksan, S. Chirachanchai, Amphiphilic chitosan nanospheres: factors to control nanosphere formation and its consequent pH responsive performance, Polymer 50 (2009) 1877–1886.
[34] A. Gupta, N. Mulchandani, M. Shah, S. Kumar, V. Katiyar, Functionalized chitosan mediated stereocomplexation of poly(lactic acid): influence on crystallization, oxygen permeability, wettability and biocompatibility behavior, Polymer 142 (2018) 196–208.
[35] H. Gu, X. Xu, H. Zhang, C. Liang, L. Han, C. Ma, Y. Li, Z. Guo, J. Gu, Chitosan-coated-magnetite with covalently grafted polystyrene based carbon nanocomposites for hexavalent chromium adsorption, Eng. Sci. 1 (2018) 46–54, www.doi.org/10.30919/espub.es.180308.
[36] M.A. Pujana, L. Pérez-Álvarez, L.C. Cesteros Iturbe, I. Katime, Water dispersible pH-responsive chitosan nanogels modified with biocompatible crosslinking-agents, Polymer 53 (2012) 3107–3116.
[37] A. Bernkop-Schnurch, S. Dunnhaupt, Chitosan-based drug delivery systems, Eur. J. Pharm. Biopharm. 81 (2012) 463–469.
[38] M.A. Elgadir, M.S. Uddin, S. Ferdosh, A. Adam, A.J.K. Chowdhury, M.Z.I. Sarker, Impact of chitosan composites and chitosan nanoparticle composites on various drug delivery systems: a review, J. Food Drug Anal. 23 (2015) 619–629.
[39] Y. Luo, Q. Wang, Recent development of chitosan-based polyelectrolyte complexes with natural polysaccharides for drug delivery, Int. J. Biol. Macromol. 64 (2014) 353–367.
[40] S. Ahmed, S. Ikram, Chitosan based scaffolds and their applications in wound healing, Achiev. life. Sci. 10 (2016) 27–37.
[41] Y. Ma, J. Dai, L. Wu, G. Fang, Z. Guo, Enhanced anti-ultraviolet, anti-fouling and anti-bacterial polyelectrolyte membrane of polystyrene grafted with trimethyl quaternary ammonium salt modified lignin, Polymer 114 (2017) 113–121.
[42] R.F.M. Elshaarawy, F.H.A. Mustafa, L. van Geelen, A.E.A. Abou-Taleb, H.R.Z. Tadros, R. Kalscheuer, C. Janiak, Mining marine shell wastes for polyelectrolyte chitosan anti-biofoulants: fabrication of high-performance economic and ecofriendly anti-biofouling coatings, Carbohydr. Polym. 172 (2017) 352–364.
[43] H.S. Lee, M.Q. Yee, Y.Y. Eckmann, N.J. Hickok, D.M. Eckmann, R.J. Composto, Reversible swelling of chitosan and quaternary ammonium modified chitosan brush layers: effect of pH and counter anion size and functionality, J. Mater. Chem. 22 (2012) 19605–19616.
[44] A. Pourjavadi, Z. Mazaheri Tehrani, S. Jokar, Chitosan based supramolecular polypseudorotaxane as a pH-responsive polymer and their hybridization with mesoporous silica-coated magnetic graphene oxide for triggered anticancer drug delivery, Polymer 76 (2015) 52–61.
[45] J. Wei, X.-J. Ju, X.-Y. Zou, R. Xie, W. Wang, Y.-M. Liu, L.-Y. Chu, Multi-Stimuli-responsive microcapsules for adjustable controlled-release, Adv. Funct. Mater. 24 (2014) 3312–3323.
[46] X. Li, P. Du, P. Liu, Novel biocompatible pH-stimuli responsive superparamagnetic hybrid hollow microspheres as tumor-specific drug delivery system, Colloids Surf., B 122 (2014) 99–106.
[47] C. Choochottiros, R. Yoksan, S. Chirachanchai, Amphiphilic chitosan nanospheres: factors to control nanosphere formation and its consequent pH responsive performance, Polymer 50 (2009) 1877–1886.
[48] A. Pourjavadi, Z. Mazaheri Tehrani, S. Jokar, Chitosan based supramolecular polypseudorotaxane as a pH-responsive polymer and their hybridization with mesoporous silica-coated magnetic graphene oxide for triggered anticancer drug delivery, Polymer 76 (2015) 52–61.
[49] M.A. Pujana, L. Pérez-Álvarez, L.C. Cesteros Iturbe, I. Katime, Water dispersible pH-responsive chitosan nanogels modified with biocompatible crosslinking-agents, Polymer 53 (2012) 3107–3116.
[50] H. Chen, C. Zhao, M. Zhang, et al., Molecular understanding and structural-based design of polyacrylamides and polyacrylates as antifouling materials, Langmuir 32 (14) (2016) 3315–3330.
[51] S.K. Samal, M. Dash, S. Van Vlierberghe, D.L. Kaplan, E. Chiellini, C. van Blitterswijk, L. Moroni, P. Dubruel, Cationic polymers and their therapeutic potential, Chem. Soc. Rev. 41 (2012) 7147–7194.
[52] D. Feng, B. Bai, H. Wang, Y. Suo, Enhanced mechanical stability and sensitive swelling performance of chitosan/yeast hybrid hydrogel beads, New J. Chem. 40 (2016) 3350–3362.
[53] X. Zou, X. Zhao, L. Ye, Q. Wang, H. Li, Preparation and drug release behavior of pH-responsive bovine serum albumin-loaded chitosan microspheres, J. Ind. Eng. Chem. 21 (2015) 1389–1397.
[54] C. Lu, B. Mu, P. Liu, Stimuli-responsive multilayer chitosan hollow microspheres via layer-by-layer assembly, Colloids Surf., B 83 (2011) 254–259.
[55] M. Prabaharan, Chitosan-based nanoparticles for tumor-targeted drug delivery, Int. J. Biol. Macromol. 72 (2015) 1313–1322.
[56] M. Andersson Trojer, L. Nordstierna, J. Bergek, H. Blanck, K. Holmberg, M. Nyden, Use of microcapsules as controlled release devices for coatings, Adv. Colloid Interface Sci. 222 (2015) 18–43.
[57] I. Bhatnagar, S.K. Kim, Immense essence of excellence: marine microbial bioactive compounds, Mar. Drugs 8 (2010) 2673–2701.
[58] D. Rittschof, Natural product antifoulants: one perspective on the challenges related to coatings development, Biofouling 15 (2000) 119–127.
[59] M. Mokhtar, G. Ginestra, F. Youcefi, A. Filocamo, C. Bisignano, A. Riazi, Antimicrobial activity of selected polyphenols and capsaicinoids identified in pepper (capsicum annuum L.) and their possible mode of interaction, Curr. Microbiol. 74 (2017) 1253–1260.
[60] J. Wang, T. Shi, X. Yang, W. Han, Y. Zhou, Environmental risk assessment on capsaicin used as active substance for antifouling system on ships, Chemosphere 104 (2014) 85–90.
[61] Q. Xu, C.A. Barrios, T. Cutright, B.M. Zhang Newby, Evaluation of toxicity of capsaicin and zosteric acid and their potential application as antifoulants, Environ. Toxicol. 20 (2005) 467–474.
[62] P.L. Nascimento, T.C. Nascimento, N.S. Ramos, G.R. Silva, J.E. Gomes, R.E. Falcao, K.A. Moreira, A.L. Porto, T.M. Silva, Quantification, antioxidant and antimicrobial activity of phenolics isolated from different extracts of Capsicum frutescens (Pimenta Malagueta), Molecules 19 (2014) 5434–5447.
[63] B. Christopher, C.E.M. Davis, Marianna A. Busch, Kenneth W. Busch, Determination of capsaicinoids in habanero peppers by chemometric analysis of UV spectral data, J. Agric. Food Chem. 55 (2007) 5925–5933.
[64] D. Zhang, Y. Fu, L. Huang, et al., Integration of antifouling and antibacterial properties in salt-responsive hydrogels with surface regeneration capacity, J. Mater. Chem. B 6 (2018) 950–960.
[65] G. Lawrie, I. Keen, B. Drew, A. Chandlertemple, L. Rintoul, P.M. Fredericks, L. Grondahl, Interactions between alginate and chitosan biopolymers characterized using FTIR and XPS, Biomacromolecules 8 (2007) 2533–2541.
[66] L. Qi, Z. Xu, X. Jiang, C. Hu, X. Zou, Preparation and antibacterial activity of chitosan nanoparticles, Carbohydr. Res. 339 (2004) 2693–2700.
[67] G. Xueli, W. Haizeng, W. Jian, H. Xing, G. Congjie, Surface-modified PSf UF membrane by UV-assisted graft polymerization of capsaicin derivative moiety for fouling and bacterial resistance, J. Membr. Sci. 445 (2013) 146–155.
[68] X. Hao, S. Chen, H. Zhu, L. Wang, Y. Zhang, Y. Yin, The synergy of graphene oxide and polydopamine assisted immobilization of lysozyme to improve antibacterial properties, Chemistry 2 (2017) 2174–2182.
[69] H. Zhu, L. Yue, C. Zhuang, Y. Zhang, X. Liu, Y. Yin, S. Chen, Fabrication and characterization of self-assembled graphene oxide/silane coatings for corrosion resistance, Surf. Coating. Technol. 304 (2016) 76–84.
[70] Z. Yang, X. Hao, S. Chen, Z. Ma, W. W, C. Wang, L. Yue, H. Sun, Q. Shao, V. Murugadoss, Z. Guo, Long-term antibacterial stable reduced graphene oxide nanocomposites loaded with cuprous oxide nanoparticles, J. Colloid. Interf. Sci. 533 (2019) 13–23.
[71] X. Hao, W. W, Z. Yang, L. Yue, H. Sun, H. Wang, Z. Guo, F. Cheng, S. Chen, pH responsive antifouling and antibacterial multilayer films with Self-healing performance, Chem. Eng. J. 356 (2019) 130–141.